

Reductions of Parvalbumin Positive Interneurons and Adult Hippocampal Neurogenesis were Observed in the Genetically Mimicked Mouse Models for *IQSEC2*-related Disorders

Mengyun ZHOU¹⁾, Qi GUO¹⁾, Emi KOUYAMA-SUZUKI¹⁾
Katsuhiko TABUCHI¹⁾²⁾* and Takuma MORI¹⁾²⁾*

- 1) *Department of Molecular and Cellular Physiology, Shinshu University School of Medicine*
2) *Department of Neuroinnovation, Institute for Biomedical Sciences, Interdisciplinary Cluster for Cutting Edge Research, Shinshu University*

Background: *IQSEC2*-related disorders are a genetic syndrome characterized by intellectual disability and various neurodevelopmental disorders. We previously generated *Iqsec2* knockout mice and conducted electrophysiological and behavioral assays to study their phenotypic manifestations. However, histological features observed in other mouse models of neurodevelopmental disorders have never been examined. We focused on the adult neurogenesis and interneuropathy as features of neurodevelopmental disorders and investigated them with the *Iqsec2* knockout mouse.

Methods: Four-month-old *Iqsec2* knockout male mice were injected with bromodeoxyuridine (BrdU) to label newly born hippocampal neurons. We estimated the number of the adult-born neurons in the hippocampus by immunohistochemistry with antibodies against BrdU and NeuN, a neuronal marker. We also quantified parvalbumin-positive neurons, a dominant subtype of GABAergic interneurons by immunohistochemistry.

Results: We observed that the number of parvalbumin interneurons decreased in the medial prefrontal cortex and the dentate gyrus of the ventral part of the hippocampus. The number of the BrdU positive neurons in the dentate gyrus of the hippocampus decreased in *Iqsec2* knockout mice. The reduction of BrdU positive neurons was observed both in the dorsal and ventral parts of the hippocampus.

Conclusion: A decrease in parvalbumin-positive neurons, occurred in the medial prefrontal cortex and the hippocampus, which indicates that a mechanism of *IQSEC2*-related disorders may involve a deficit of interneurons. Considering that adult neurogenesis seems important for cognitive brain functions, a reduction of adult-born neurons in the hippocampus may be related to some of the phenotypes of *IQSEC2*-related disorders, such as intellectual disability. *Shinshu Med J* 72 : 385—396, 2024

(Received for publication August 8, 2024 ; accepted in revised form August 23, 2024)

Key words: *IQSEC2*-related disorders, adult neurogenesis, interneuron, neurodevelopmental disorders

Abbreviations: PV neuron, parvalbumin positive neuron ; BrdU, Bromodeoxyuridine ; VPA, valproic acid ; PNE, prenatal nicotine exposure ; *IQSEC2*, IQ motif and Sec7 domain 2 ; ASD, autism spectrum disorders ; GABA, gamma amino butyric acid ; PBS, phosphate buffered saline ; AAV, adeno-associated virus

* Corresponding author : Katsuhiko Tabuchi and Takuma Mori
Department of Molecular and Cellular Physiology,
Shinshu University School of Medicine, 3-1-1 Asahi,
Matsumoto, Nagano 390-8621, Japan
Department of Neuroinnovation, Institute for Biomedical
Sciences, Interdisciplinary Cluster for Cutting Edge
Research, Shinshu University, 3-1-1 Asahi, Matsumoto,
Nagano 390-8621, Japan
Email : ktabuchi@shinshu-u.ac.jp, mori@shinshu-u.ac.jp

I Introduction

IQ motif and Sec7 domain 2 (*IQSEC2*, aka BRAG1) is a guanine nucleotide exchange factor for ADP-ribosylation factors (GEF-Arfs), constituting a IQSEC protein family together with *IQSEC1* and *IQSEC3*. *IQSEC2* has been reported to activate Arf6 specifically by exchanging its guanosine diphosphate (GDP)

to guanosine triphosphate (GTP)¹⁾. Recent studies have highlighted the significance of Arf6 in the development and maturation of synapses. Arf6 activated by IQSEC2 is involved in the trafficking of synaptic vesicles, the formation of dendritic spines, and the regulation of receptor recycling, processes that are critical for the proper functioning of synapses²⁾. IQSEC2 is localized at excitatory glutamatergic synapses together with postsynaptic molecules such as NMDA and AMPA receptors, and PSD-95³⁾⁻⁵⁾.

The *IQSEC2* gene is located on Xp11.22 in human and mutations in *IQSEC2* have been linked to a spectrum of neurodevelopmental disorders, including non-syndromic X-linked intellectual disability and Autism Spectrum Disorder (ASD)⁶⁾. The inheritance pattern of the *IQSEC2*-related disorders (#MIM 309530) is complex because the *IQSEC2* gene is known to escape X chromosome inactivation⁷⁾. Epilepsy is a common phenotype and 70 % of females and 90 % of males were affected by *IQSEC2*-encephalopathy and the prevalence of the *IQSEC2*-encephalopathy was estimated to be 0.00007/100,000 in an Italian population⁸⁾. The authors reported more than 70 % of patients showed a severe degree of intellectual disability in both sexes and ASD-like features such as the impairment of social interaction and restrictive and repetitive behaviors. A brain MRI study reported abnormal findings including white matter changes, thin corpus callosum, and cortical atrophy⁹⁾.

These pathogenic variants can lead to either loss of function or gain of function, disrupting normal synaptic signaling and plasticity, which are critical for cognitive processes such as learning and memory¹⁰⁾. There have been several mouse models of *IQSEC2*-related disorders developed and investigated the pathological phenotypes¹¹⁾⁻¹⁴⁾. One of these four *Iqsec2* mutant mice carries a missense pathogenic variant of *Iqsec2* gene, A350V, which was identified in a patient caused by *IQSEC2*-related disorders¹³⁾ and the other three lines are *Iqsec2* knockout mice. These *Iqsec2* knockout mice shared common phenotypes, such as the hyperactivity during the open field test¹¹⁾¹²⁾¹⁴⁾, and the reduction of social interactions evaluated by three chamber test¹¹⁾ or ultrasonic vocalization test¹²⁾.

While the genetic and environmental factors contributing to neurodevelopmental disorders are complex, recent research has identified specific neural circuits and cell types that play pivotal roles in their pathogenesis¹⁵⁾. Among these, parvalbumin positive (PV) neurons, a subtype of GABAergic interneurons, have garnered significant attention due to their crucial role in maintaining the balance of excitation and inhibition in the brain¹⁶⁾. PV neurons are characterized by their expression of the calcium-binding protein parvalbumin and are predominantly found in the cortex and hippocampus¹⁷⁾. These fast-spiking interneurons are essential for the synchronization of neuronal networks and the generation of gamma oscillations, which are critical for cognitive processes such as perception, attention, and memory¹⁸⁾. Disruption in the function or development of PV neurons has been implicated in various neurodevelopmental disorders, suggesting that these neurons are key players in the pathophysiology of these conditions. Alterations in inhibitory interneuron function have been reported in *Iqsec2* knockout mice, including an increase in inhibitory neurotransmission and in the number of PV neurons in the hippocampus¹²⁾. In contrast, we previously observed a decrease in inhibitory neurotransmission in the neocortex¹¹⁾, but we did not examine the distribution of PV neurons in the mouse brain.

Adult neurogenesis, the process by which new neurons are generated in the adult brain, occurs primarily in two regions: the subgranular zone of the hippocampal dentate gyrus and the subventricular zone lining the lateral ventricles. Dysregulation of adult neurogenesis has been implicated in a variety of neurodevelopmental disorders, suggesting that this process is crucial for maintaining normal brain function¹⁹⁾²⁰⁾. For example, pathogenic variants in genes involved in neural stem cell proliferation and differentiation, such as *DISC1* (Disrupted in Schizophrenia 1) and *FMRI* (Fragile X Mental Retardation 1), can impair adult neurogenesis and contribute to the pathology of schizophrenia and Fragile X syndrome, respectively²¹⁾⁻²³⁾. To date, adult neurogenesis has never been investigated in any of *Iqsec2* mutant mice.

We previously generated an *Iqsec2* knockout mouse and identified altered neurophysiological and behavioral functions¹¹. The mouse model exhibited the reduction of excitatory glutamatergic and inhibitory GABAergic neurotransmissions and the impairments of social behaviors, indicating that the *Iqsec2* knockout mouse can be an animal model of *IQSEC2*-related disorders. The histological features observed in other ASD models, such as PV and adult-born neurons, have never been examined in this *Iqsec2* knockout mouse. In the current study, we assessed the distribution of PV neurons and adult-born neurons in the brain of *Iqsec2* knockout mice and found that the numbers of PV neurons in the medial prefrontal cortex and adult-born neurons in the hippocampus decreased in the *Iqsec2* knockout mouse. These results indicate that the deficiency of *Iqsec2* gene in the mouse causes an alteration of the neuronal structure.

II Materials and Methods

A Ethics

All procedures of the animal experiments were reviewed by the Committee for Animal Experiments of Shinshu University and approved by the president of Shinshu University (Approved number #021045). Mice were group-housed under environmentally controlled conditions (12:12 light/dark cycle, 22 ± 2 °C, and 55 ± 10 % relative humidity) with food and water ad libitum.

B *Iqsec2* knockout mice

Iqsec2 knockout mice were generated previously using CRISPR/Cas9-based genome-editing via electroporation¹¹. Briefly, a ribonucleoprotein complex of single-guide RNA (aka crRNA) targeting exon 3 of *Iqsec2* gene, tracrRNA, and Cas9 protein were electroporated into fertilized eggs of C57BL/6JmsSlc mice (Japan SLC) by using a NEPA21 electroporator (Nepa Gene). The electroporated embryos were transferred to the oviduct of a surrogate mother of ICR strain (Japan SLC). We screened a mouse with 17-bp-deletion in exon 3 of *Iqsec2* gene by Sanger sequencing, resulting in D255X nonsense pathogenic variant of *Iqsec2* gene (**Fig. 1A**). The mice were maintained on a hybrid background of C57BL/6JmsSlc

and 129+TerSvJcl. The mice used in this study were genotyped using two pairs of primers to distinguish between wild-type and knockout mice. For wild-type mice, the primers used were 5'-TTGAGTGAATGAACCGTGTAG-3' and 5'-ATCAACCGCTGTGCTCAGGTC-3'. For *Iqsec2* knockout mice, the primers used were 5'-TTGAGTGAATGAACCGTGTAG-3' and 5'-CCAGGACTATCAACTGCCTG-3'. All the experimenters were blinded either to the genotype or phenotype of the mice throughout the study.

C Prediction of the structure of IQSEC2

The structure of IQSEC2 protein was predicted using AlphaFold3 algorithm²⁴ on the AlphaFold server beta (<https://alphafoldserver.com>). We provided a FASTA sequence (NP_001108136.1) to the AlphaFold server as an input and analyzed the model_0 on PyMOL software (Retrieved from <http://www.pymol.org/pymol>). pLDDT of the predicted structure of IQSEC2 protein was colored using a PyMOL plugin (<https://github.com/YoshitakaMo/pymol-psico>).

D Immunohistochemistry for PV neurons

Histological procedures were followed according to our previous protocols²⁵⁾²⁶. The mice were approximately 4-month-old, when the neurological issues like seizure and sudden death were reported to be stabilized in knockout mice¹⁴. The mice were deeply anesthetized with an anesthesia cocktail including dexmedetomidine hydrochloride (0.3 mg/kg BW), midazolam (4 mg/kg) and butorphanol tartrate (5.0 mg/kg) and perfused with ice-cold phosphate buffered saline (PBS) followed by 4 % paraformaldehyde in PBS. The brain was sampled and postfixed in 4 % PFA in PBS overnight and put in 30 % sucrose in PBS until it sank. The brains were cut into thin slices of forty μ m thickness. The brain slices were kept in Cryoprotectant (30 % sucrose, 1 % polyvinyl-pyrrolidone-40, 30 % ethylene glycol in 0.1M phosphate buffer, pH 7.4) at -20 °C. The brain slices were pre-washed in PBS and incubated in blocking buffer (0.25 % Triton X-100 and 10 % normal donkey serum) for 1 hour at room temperature. After blocking, the brain slices were washed in PBS containing 0.005 % Tween-20 (PBST) and incubated with mouse anti-parvalbumin mono-

clonal antibody (PV-19, Sigma-Aldrich, 1:1000 dilution) at 4 °C overnight. After washing in PBST, the brain slices were incubated with a secondary donkey-antibody against mouse IgG conjugated with Alexa 594 (Thermo Fisher, 1:1000 dilution). After further washing, the brain slices were counterstained with DAPI and mounted on slides and coverslipped. Fluorescence imaging was conducted using a fluorescent microscope (BZ-X800, Keyence) and a confocal laser-scanning microscope (TCS SP8, Leica Microsystems). For each brain region analyzed, an average of 3 brain slices per mouse were examined, with six animals analyzed per group. Regions of interest were delineated using clearly visible landmarks and predefined boundaries according to the Allen Brain Atlas.

E BrdU injection and visualization of adult-born neurons

BrdU was administered to approximately 4 month-old eight wild-type and six *Iqsec2* knockout mice following a previously established protocol²⁷. Mice received intraperitoneal injections of BrdU (150 mg/kg) three times daily for five consecutive days. Serial coronal sections (40 μm thickness) were cut using a freezing microtome. Sections were initially washed in PBS for 15 minutes. For BrdU detection, DNA was denatured by incubating sections in 1M HCl for 30 minutes at 37 °C, followed by neutralization in PBS (5 minutes, three times). Sections were then incubated in a blocking solution containing 10 % donkey serum and 0.3 % Triton X-100 in PBS for 1 hour at room temperature. Primary antibodies, mouse anti-NeuN (1:1000, MAB377, Roche) and rat anti-BrdU (1:200, ab6326, Abcam), were applied overnight at 4 °C. After washing in PBS (5 minutes, three times), sections were incubated with secondary antibodies (Alexa-488-conjugated donkey anti-mouse IgG and Alexa-594-conjugated donkey anti-rat IgG, both at 1:400, Thermo) for 2-3 hours at room temperature in the dark. Sections were counterstained with DAPI, mounted and coverslipped.

Mice were perfused two weeks after the last BrdU administration in the same method described above. Coronal brain sections were imaged using a confocal microscope (SP8, Leica) or a fluorescent microscope

(BZ-X800, Keyence) equipped with a 10× objective lens. Images were stitched using Keyence Image Analyzer software (v. 1.1.2.4). To cover the entire hippocampal formation, every sixth section was selected. Sections located anterior to bregma -2.80 mm were categorized as the dorsal DG, while sections posterior to this point were categorized as the ventral DG. Newborn neurons were identified as cells positive for both NeuN and BrdU. The total number of these double-positive cells was counted within the dentate gyrus. To estimate the total number of newborn neurons, the average number of double-positive cells per section (total counted cells divided by the number of sections counted) was multiplied by the total number of sections encompassing the hippocampal region (approximately 36 sections for the dorsal and 36 for the ventral DG).

F Estimation of the hippocampal volume

The hippocampus and its subfields (CA1 and the dentate gyrus) were identified and outlined from the micrographs and their areas were measured using ImageJ 2.14.0. This measurement was performed for each slice of the brain. The volume of the hippocampus was estimated using the formula :

$$V = t \times \sum_{i=1}^n A_i$$

where V is the total volume, t is the thickness of each slice, n is the total number of slices, and A_i is the area of the hippocampus in the i -th slice. The volumes of each subfield and the whole dorsal hippocampus were then calculated. All measurements were performed bilaterally, and the total hippocampal volume for each brain was obtained by summing the volumes of all slices.

G Statistical analysis

Sample sizes were determined based on established practice and on our previous experience in respective assays. All values represent the average of independent experiments \pm SEM. The variance among analyzed samples was similar. Statistical significance was determined by Student's t -test. Statistical analysis was performed using GraphPad Prism 8 and custom-written R scripts. Statistical significance was indicated by asterisks ($*p < 0.05$, $**p < 0.01$). All data were expressed as means \pm SEM.

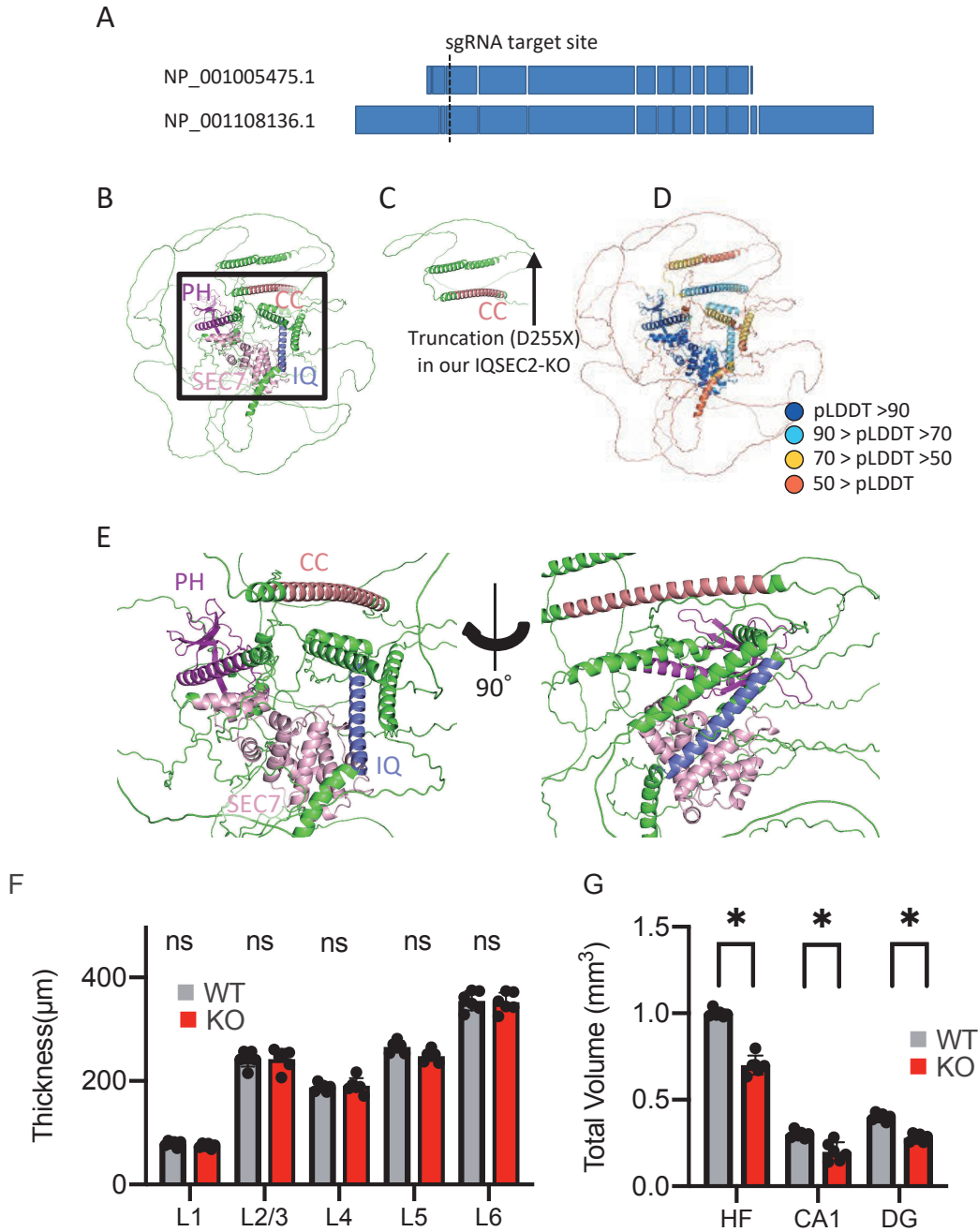


Fig. 1 Protein Structure of IQSEC2 in wild-type and knockout mice

Panel A, two major isoforms of the mouse IQSEC2 protein. The target site used in this study was shown by a dashed line. Rectangles indicate exons of *IQSEC2* gene. Panel B, a predicted protein structure of mouse IQSEC2 by AlphaFold3. Four functional domains were colored differently from other part of IQSEC2 protein. Panel C, truncated IQSEC2 protein in our *Iqsec2* knockout mouse, Panel D, pLDDT scores of predicted IQSEC2 protein, indicating local structure of functional domains were predicted with a high accuracy. Panel E, microscopic view of the IQSEC2 functional domains, indicated by a rectangle in the Panel B. Panel F, the thickness of cortical layers of the somatosensory cortex. No difference was observed between wild-type (grey) and *Iqsec2* knockout (red) mice. Panel G, the volume of the hippocampal formation of the mice. The volume decreased in *Iqsec2* knockout in comparison with the wild-type mouse. HF, hippocampal formation. Asterisks indicate a statistically significant difference by student's t-test (* $p < 0.05$).

III Results

A Genomic and protein structures of mouse *Iqsec2*

We previously generated the *Iqsec2* knockout mice using CRISPR/Cas9-based genome editing¹¹ and found the mouse expresses a truncated *Iqsec2* (Fig. 1A,

D255X nonsense pathogenic variant). We used AlphaFold3 to predict the structure of *Iqsec2* (**Fig. 1B**) and confirmed our previous result that the part remained by the truncation contained only coiled-coil domain but no other functional domains such as IQ-motif and Sec7 domain (**Fig. 1C**). The four primary functional domains of *Iqsec2* protein were predicted with relatively high confidence (pLDDT>70) by AlphaFold3 (**Fig. 1D**). These four domains were predicted to be located close to each other, indicating that these domains could work in cooperation in wild-type animals (**Fig. 1E**).

Additionally, we evaluated the overall brain morphology in the knockout mice. Quantitative analysis of the neocortex showed no significant changes in the thickness of the somatosensory cortex layers (**Fig. 1F**). However, volumetric measurements revealed a significant reduction in the hippocampal formation and its subregions, including CA1 and the dentate gyrus, in *Iqsec2* knockout mice compared to wild-type controls (**Fig. 1G**).

B Distribution of PV neurons between wild-type and *Iqsec2* knockout mice

Given our previous finding of reduced inhibitory GABAergic neurotransmission in the medial prefrontal and somatosensory cortices¹¹, we further investigated the potential histological alterations in these regions by examining the distribution of PV neurons, which consist of a major subtype of GABAergic inhibitory interneurons in the neocortex. We examined the cell density of PV neurons in the medial prefrontal cortex (**Fig. 2A, B**) and the somatosensory cortex (**Fig. 2C, D**). We separated the medial prefrontal cortex into three sub-regions, the cingulate area 1 (Cg1), the prelimbic (PrL), and the infralimbic (IL) based on the Allen Brain Atlas and we found that the cell-density of PV neurons decreased in PrL and the IL of *Iqsec2* knockout mice. The cell density of PV neurons in the medial prefrontal cortex (**Fig. 2A**) was decreased significantly in prelimbic and infralimbic regions (**Fig. 2B**). We also investigated the cell density of PV neurons in the somatosensory cortex of *Iqsec2* knockout mice (**Fig. 2C**). The cell density of PV neurons, on the other hand, did not decrease in

the somatosensory cortex (**Fig. 2D**). We next examined the cell density of PV neurons in the hippocampus (**Fig. 3A, B**). We found a reduction of PV neurons in the dentate gyrus of the ventral part, but not the dorsal part, of the hippocampus (**Fig. 3C**). The cell density of PV neurons was not altered in the CA1 region of the hippocampus (**Fig. 3D**).

C Adult neurogenesis decreased in the hippocampus of *Iqsec2* knockout mice

Recent researchers have shown that adult neurogenesis in the hippocampus is associated with cognitive functions such as learning and spatial memory, as well as emotional behaviors²⁸. We previously demonstrated that adult neurogenesis was decreased in prenatal nicotine exposure (PNE) mice, a model of neurodevelopmental disorders²⁷. We investigated the number of the adult-born neurons, which are defined as double positive cells for BrdU and neuronal nuclear protein (NeuN), in the *Iqsec2* knockout mice (**Fig. 4A**). We separated the hippocampus into two sub divisions, dorsal and ventral parts, which are related to spatial and emotional behaviors, respectively²⁹. We observed that the number of adult-born neurons decreased in *Iqsec2* knockout mice than in wild-type neurons by approximately 40 % (**Fig. 4B**). The reduction in adult-born neurons was observed not only in the ventral part of the hippocampus but also in the dorsal part, which is different from the finding in PNE mice we reported previously²⁷.

IV Discussion

In the present study, we assessed the distribution of PV neurons and adult-born neurons in *Iqsec2* knockout mice and found that PV neurons and adult-born neurons decreased in *Iqsec2* knockout mice.

We previously examined electrophysiological and behavioral characteristics of *Iqsec2* knockout mice, which showed alterations of synaptic neurotransmission and social behaviors¹¹. In the study, we demonstrated that the reduction of GABAergic inhibitory neurotransmissions on the pyramidal neurons in the neocortex. The findings in the current study support the previous physiological data, considering that PV neurons is a major subpopulation of GABAergic in-

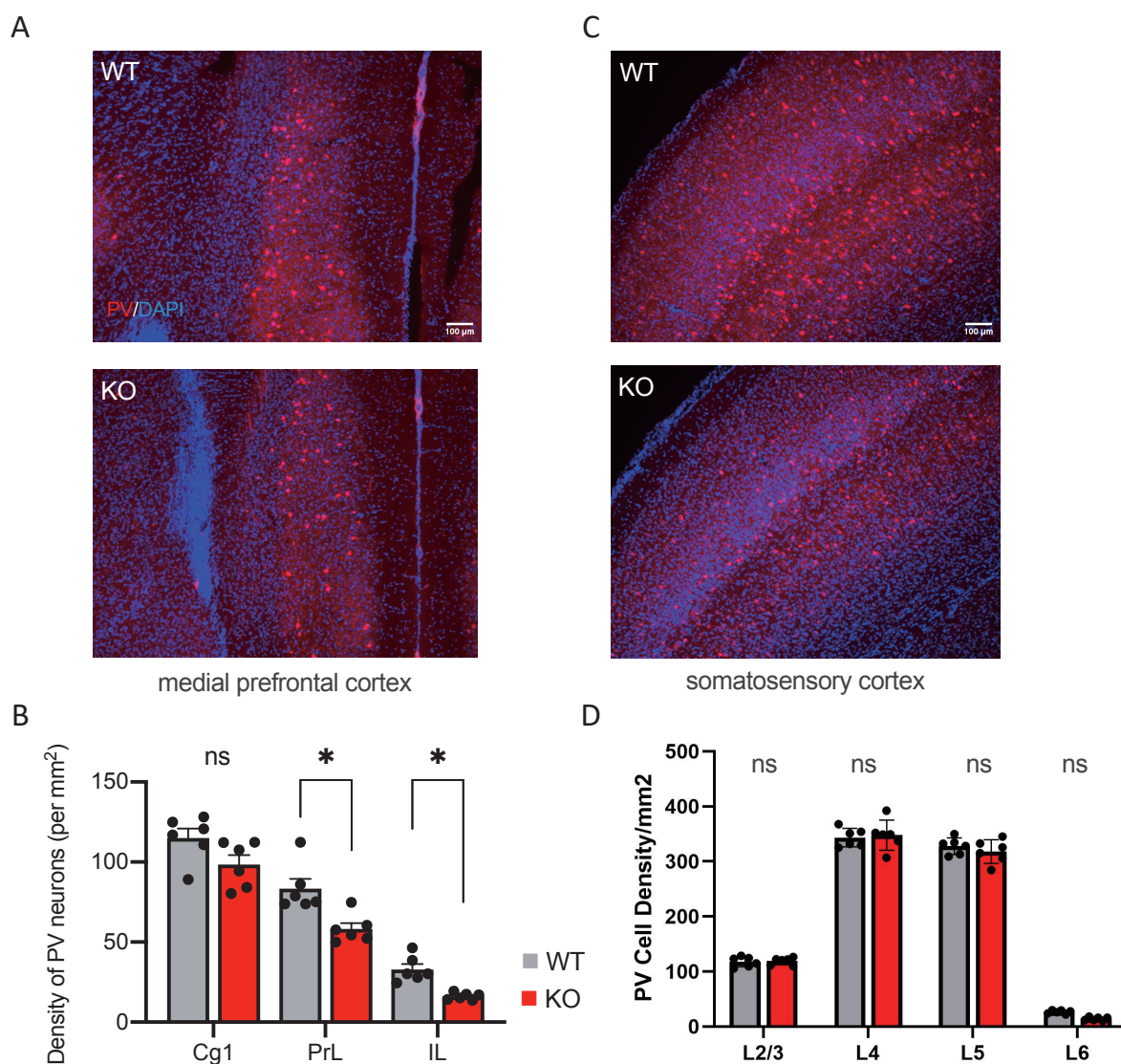


Fig. 2 Parvalbumin distribution in the neocortical regions of wild-type and *Iqsec2* knockout mice

Panel A, histochemical images of parvalbumin (PV) immune-positive neurons (red) in the medial prefrontal cortex. The structure of the brain was visualized by the counter-staining with DAPI (blue). Scale bar indicates 100 μm . Panel B, quantitative analysis of the cell density of PV cells in sub-regions of the medial prefrontal cortex. The subregions are cingulate area 1 (Cg1), prelimbic area (PrL), and infralimbic area (IL). Data from wild-type (grey bars) and *Iqsec2* knockout (red) mice, and data from each animal indicate with dots. Panel C, images of PV cells in the somatosensory cortex of wild-type and *Iqsec2* knockout mice. Panel D, quantitative analysis of PV cell density on the somatosensory cortex is shown. Asterisks indicate statistically significant difference detected by Student's t-test (* $p < 0.05$).

inhibitory interneurons. In addition to our knockout mouse, *Iqsec2* knockout mice were established and examined by Sah et al.¹²). They reported there was no alteration in glutamatergic excitatory neurotransmission but an increase in GABAergic inhibitory neurotransmission in the hippocampal neuron culture. They also observed that the number of PV neurons increased in the hippocampus, which support their

electrophysiological findings. There are possible reasons to cause these differences. One of the possible reasons is the difference of the animal strain used to establish *Iqsec2* knockout mice. We used a hybrid background of C57BL/6JmsSlc and 129+TerSvJcl because they have a better maternal care for pups, whereas they used the C3HeB/FeJ and C57BL/6NJ strains for the same reason. It is known that the back-

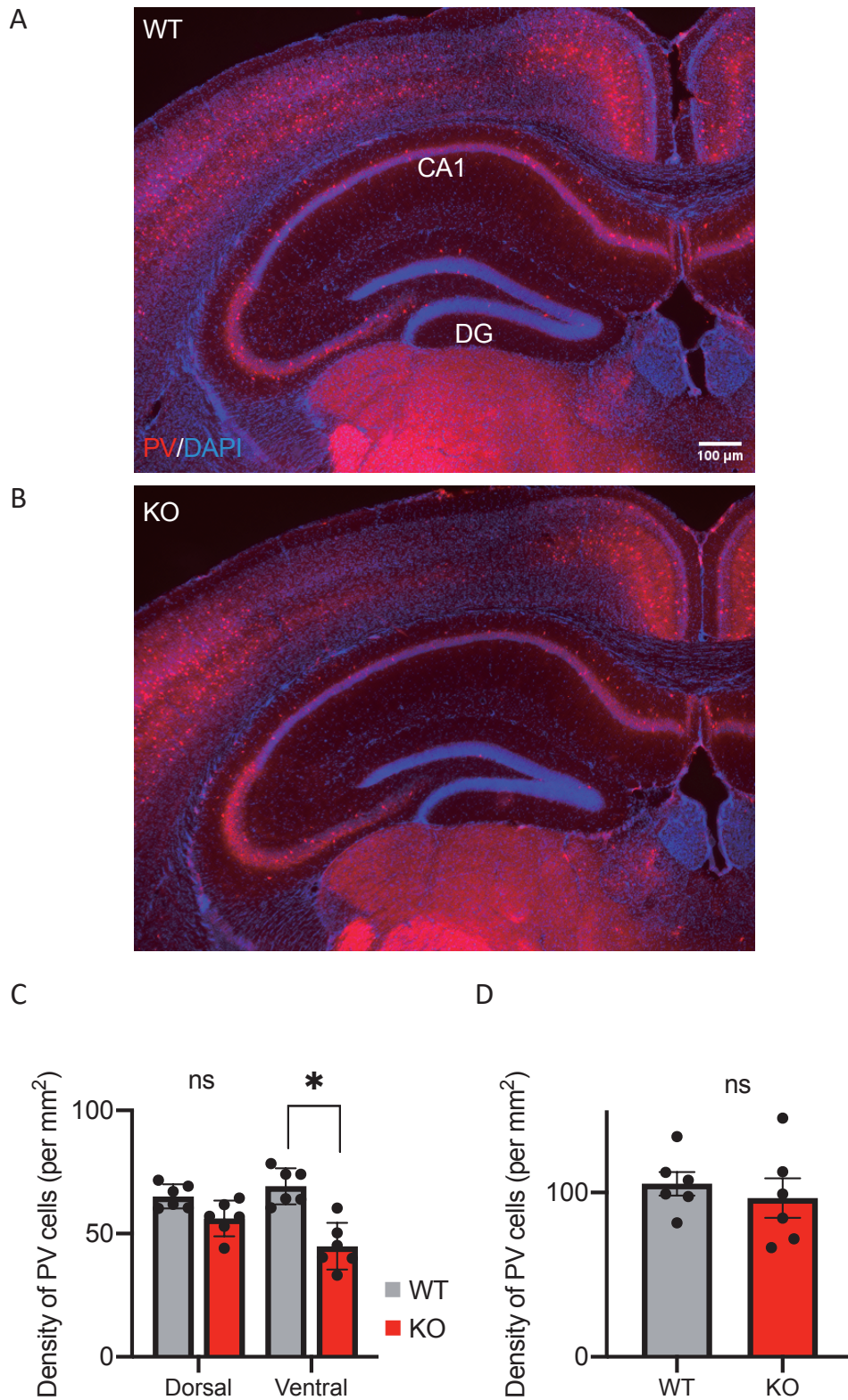


Fig. 3 Parvalbumin distribution in the hippocampus of wild-type and *Iqsec2* knockout mice

Panel A, histochemical images of parvalbumin (PV) immune-positive neurons (red) in the hippocampus, counter-stained with DAPI (blue). Scale bar indicates 100 μ m. Panel B, quantitative analysis of the cell density of PV cells in the dentate gyrus of the hippocampus. Data from wild-type (grey bars) and *Iqsec2* knockout (red) mice, and data from each animal indicate with dots. Panel C, images of PV cells in CA1 of the hippocampus of wild-type and *Iqsec2* knockout mice. Asterisk indicates statistically significant difference detected by Student's t-test (* p <0.05).

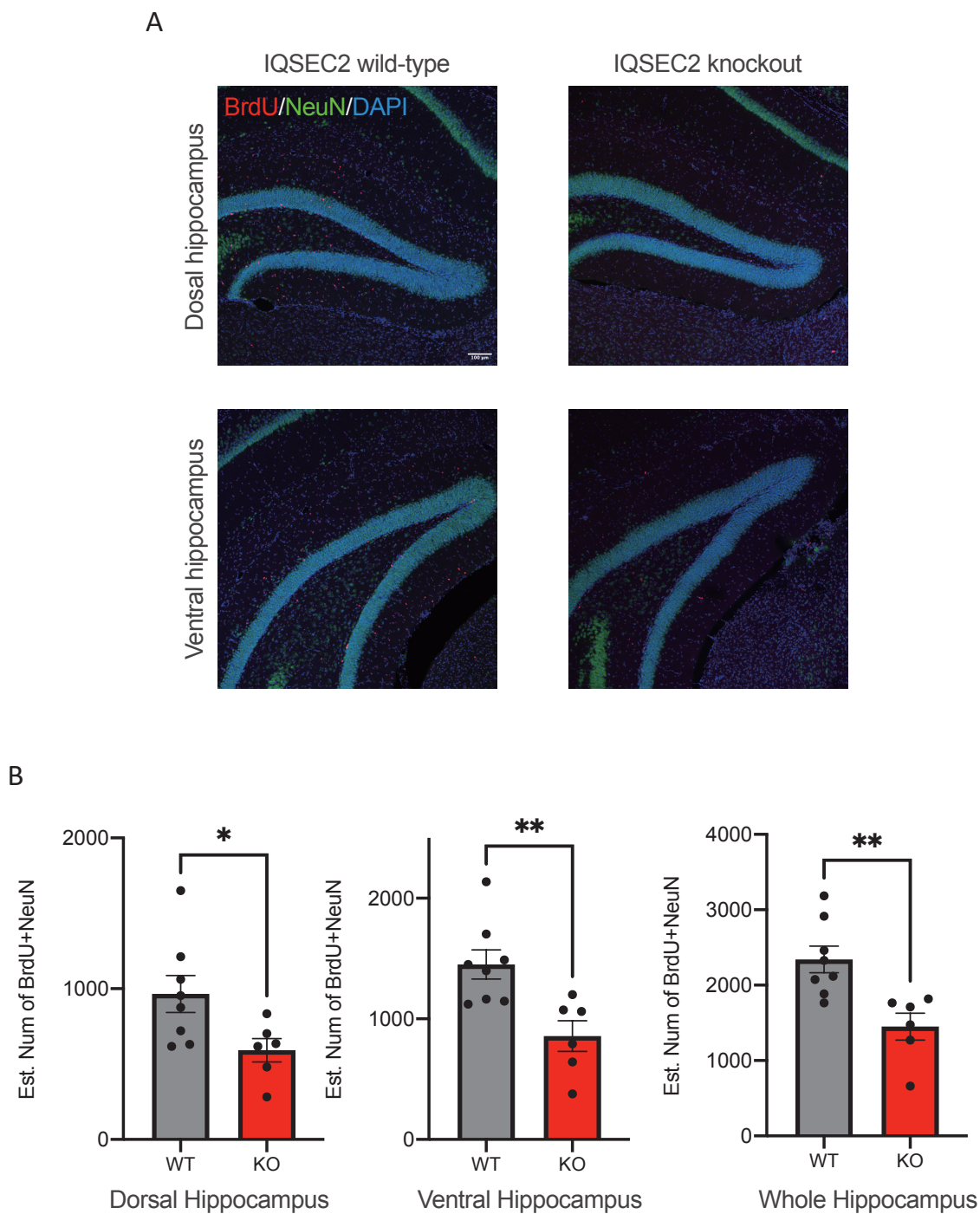


Fig. 4 Adult neurogenesis in the dentate gyrus of the hippocampus of wild-type and *Iqsec2* knockout mice
 Panel A, adult-born neurons were visualized by BrdU (red) and brain sections were stained with anti-NeuN antibody (green) and DAPI (blue). Scale bar indicates 100 μm . Panel B, estimated number of adult-born neurons, BrdU and NeuN double positive cells, decreased in the dorsal and ventral parts of the hippocampus in *Iqsec2* knockout mice. Asterisks indicate statistically significant differences between wild-type and *Iqsec2* knockout mice (* $p < 0.05$; ** $p < 0.01$, by student's t-test).

ground strains of the mouse affect the neural and biological characteristics. For example, our mice survive more than one year, but the other *Iqsec2* knock-

out mice die before 187 days old¹²). Pathogenic variants we introduced and the age we analyzed were different from their studies. These may also cause

the different results.

We found that adult-born neurons in the hippocampus decreased both in the dorsal and ventral hippocampus of the *Iqsec2* knockout mice. The decrease in adult neurogenesis in the hippocampus has been reported in several lines of ASD models such as the PNE mice, which we reported previously²⁷⁾. In the current study, however, we found the reduction of adult neurogenesis occurred in both the ventral and dorsal parts of the hippocampus, whereas the reduction occurred only in the ventral part of the hippocampus of the PNE mouse²⁷⁾. In addition to our previous report, the reduction of the adult neurogenesis was found also in another mouse model of ASD with a missense pathogenic variant on *Nlgn3* gene³⁰⁾. There are several possibilities that explain the discrepancy among these studies. We used approximately 4-month-old animals in this study, but 2-month-old animals were used in the previous studies. Adult neurogenesis is regulated not only by the genetic factors, but also by the age or the environmental conditions³¹⁾ and the adult neurogenesis is known to decrease during aging. We found decreased number of adult-born neurons in the current study (~2,500 neurons) than the previous study (~7,500 neurons), even in wild-type animals. We used the same method to label adult-born neurons in the studies, indicating the reduction of adult neurogenesis may be caused by the ages of the animals. The severity of the phenotypes of these mouse models may also be the reason. The *Iqsec2* gene is known to cause different severe phenotypes in human by nonsense and missense pathogenic variants³²⁾ and PNE cause milder phenotypes such as ADHD and ASD in most of the cases³³⁾. More fundamental effects may be caused by the deficiency of *Iqsec2* gene than PNE. Therefore, the combinational effects of *Iqsec2* pathogenic variant and the age of the animals may cause the difference. To answer the question whether the patterns of adult neurogenesis may be a common phenotype throughout neurodevelopmental disorders, more animal models must be examined in future studies.

The electrophysiological and behavioral phenotypes of *Iqsec2* knockout mice were rescued by the adeno-

associated virus (AAV)-mediated transfer of *Iqsec2* gene to the medial prefrontal cortex. The AAV-mediated gene transfer has been examined and succeeded to ameliorate the pathological phenotypes in model animals of Rett syndrome and FOXP1-related disorders³⁴⁾³⁵⁾. Since the differentiation and the localization of PV neurons were determined at early embryonic stages³⁶⁾, the genetic transfer of *Iqsec2* gene may not rescue the PV neurons. On the other hand, the reduction of adult neurogenesis may be recovered because adult neurogenesis is continuous event throughout the life. Adult neurogenesis has been reported to be rescued by the supplementation of some drugs, such as fluoxetine³⁰⁾. Therefore, AAV-mediated transfer may ameliorate the alteration of adult neurogenesis.

Disclosure

No author has an actual or perceived conflict of interest regarding the contents of this article.

Acknowledgements

We thank all the Tabuchi-lab members for generous supports on this study. MZ, TM and KT conceived the original idea of this study. MZ performed all the experiments. TM used AlphaFold3 to predict IQSEC2 protein structure. QG and EK helped to prepare animals for blind experiments (independent genotyping). MZ and KT wrote the manuscript with helps by the other co-authors.

Funding information

This work was supported by grants KAKENHI 23H02575 (K.T.), the Grant-in-Aid for Transformative Research Areas (A) (23H04227 to K.T.); JST SPRING, Grant Number JPMJSP2144 (Shinshu University to M.Z.); the IQSEC2 Research and Advocacy Foundation Research Grant Program (#2024-02 to T.M.); the Takeda Science Foundation (K.T.); and SENSHIN Medical Research Foundation (K.T.).

References

- 1) Um JW : Synaptic functions of the IQSEC family of ADP-ribosylation factor guanine nucleotide exchange factors. *Neurosci Res* 116 : 54-59, 2017
- 2) Sakagami H, Sanda M, Fukaya M, et al : IQ-ArfGEF/BRAG1 is a guanine nucleotide exchange factor for Arf6 that interacts with PSD-95 at postsynaptic density of excitatory synapses. *Neurosci Res* 60 : 199-212, 2008
- 3) Frank RAW, Zhu F, Komiyama NH, Grant SGN : Hierarchical organization and genetically separable subfamilies of PSD95 postsynaptic supercomplexes. *J Neurochem* 142 : 504-511, 2017
- 4) Elagabani MN, Brisevac D, Kintscher M, et al : Subunit-selective N-Methyl-d-aspartate (NMDA) Receptor Signaling through Brefeldin A-resistant Arf Guanine Nucleotide Exchange Factors BRAG1 and BRAG2 during Synapse Maturation. *J Biol Chem* 291 : 9105-9118, 2016
- 5) Murphy JA, Jensen ON, Walikonis RS : BRAG1, a Sec7 domain-containing protein, is a component of the postsynaptic density of excitatory synapses. *Brain Res* 1120 : 35-45, 2006
- 6) Shoubridge C, Tarpey PS, Abidi F, et al : Mutations in the guanine nucleotide exchange factor gene IQSEC2 cause nonsyndromic intellectual disability. *Nat Genet* 42 : 486-488, 2010
- 7) Tukiainen T, Villani AC, Yen A, et al : Landscape of X chromosome inactivation across human tissues. *Nature* 550 : 244-248, 2017
- 8) Leoncini S, Boasiako L, Lopergolo D, et al : Natural Course of. *Children (Basel)* 10, 2023 Leoncini S, Boasiako L, Lopergolo D, et al : Natural Course of IQSEC2-Related Encephalopathy : An Italian National Structured Survey. *Children (Basel)* 10 : 1442, 2023
- 9) Zerem A, Haginoya K, Lev D, et al : The molecular and phenotypic spectrum of IQSEC2-related epilepsy. *Epilepsia* 57 : 1858-1869, 2016
- 10) Shoubridge C, Walikonis RS, Gecz J, Harvey RJ : Subtle functional defects in the Arf-specific guanine nucleotide exchange factor IQSEC2 cause non-syndromic X-linked intellectual disability. *Small GTPases* 1 : 98-103, 2010
- 11) Mehta A, Shirai Y, Kouyama-Suzuki E, et al : IQSEC2 Deficiency Results in Abnormal Social Behaviors Relevant to Autism by Affecting Functions of Neural Circuits in the Medial Prefrontal Cortex. *Cells* 10 : 2724, 2021
- 12) Sah M, Shore AN, Petri S, et al : Altered excitatory transmission onto hippocampal interneurons in the IQSEC2 mouse model of X-linked neurodevelopmental disease. *Neurobiol Dis* 137 : 104758, 2020
- 13) Rogers EJ, Jada R, Schragenheim-Rozales K, et al : An IQSEC2 Mutation Associated With Intellectual Disability and Autism Results in Decreased Surface AMPA Receptors. *Front Mol Neurosci* 12 : 43, 2019
- 14) Jackson MR, Loring KE, Homan CC, et al : Heterozygous loss of function of IQSEC2/ Iqsec2 leads to increased activated Arf6 and severe neurocognitive seizure phenotype in females. *Life Sci Alliance* 2 : e201900386, 2019
- 15) Exposito-Alonso D, Rico B : Mechanisms Underlying Circuit Dysfunction in Neurodevelopmental Disorders. *Annu Rev Genet* 56 : 391-422, 2022
- 16) Yizhar O, Fenno LE, Prigge M, et al : Neocortical excitation/inhibition balance in information processing and social dysfunction. *Nature* 477 : 171-178, 2011
- 17) Antoine MW, Langberg T, Schnepel P, Feldman DE : Increased Excitation-Inhibition Ratio Stabilizes Synapse and Circuit Excitability in Four Autism Mouse Models. *Neuron* 101 : 648-661 e644, 2019
- 18) Sohal VS, Zhang F, Yizhar O, Deisseroth K : Parvalbumin neurons and gamma rhythms enhance cortical circuit performance. *Nature* 459 : 698-702, 2009
- 19) Adhya D, Swarup V, Nagy R, et al : Atypical Neurogenesis in Induced Pluripotent Stem Cells From Autistic Individuals. *Biol Psychiatry* 89 : 486-496, 2021
- 20) Marchetto MC, Belinson H, Tian Y, et al : Altered proliferation and networks in neural cells derived from idiopathic autistic individuals. *Mol Psychiatry* 22 : 820-835, 2017

- 21) Duan X, Chang JH, Ge S, et al: . Disrupted-In-Schizophrenia 1 regulates integration of newly generated neurons in the adult brain. *Cell* 130 : 1146-1158, 2007
- 22) Eadie BD, Zhang WN, Boehme F, et al: Fmr1 knockout mice show reduced anxiety and alterations in neurogenesis that are specific to the ventral dentate gyrus. *Neurobiol Dis* 36 : 361-373, 2009
- 23) Mahoney HL, Bloom CA, Justin HS, et al: DISC1 and reelin interact to alter cognition, inhibition, and neurogenesis in a novel mouse model of schizophrenia. *Front Cell Neurosci* 17 : 1321632, 2023
- 24) Abramson J, Adler J, Dunger J, et al: Accurate structure prediction of biomolecular interactions with AlphaFold 3. *Nature* 630 : 493-500, 2024
- 25) Badawi M, Mori T, Kurihara T, et al: Risperidone Mitigates Enhanced Excitatory Neuronal Function and Repetitive Behavior Caused by an ASD-Associated Mutation of SIK1. *Front Mol Neurosci* 14 : 706494, 2021
- 26) Pang B, Mori T, Badawi M, et al: An Epilepsy-Associated Mutation of Salt-Inducible Kinase 1 Increases the Susceptibility to Epileptic Seizures and Interferes with Adrenocorticotrophic Hormone Therapy for Infantile Spasms in Mice. *Int J Mol Sci* 23 : 7927, 2022
- 27) Zhou M, Qiu W, Ohashi N, et al: Deep-Learning-Based Analysis Reveals a Social Behavior Deficit in Mice Exposed Prenatally to Nicotine. *Cells* 13 : 275, 2024
- 28) Anacker C, Hen R: Adult hippocampal neurogenesis and cognitive flexibility-linking memory and mood. *Nat Rev Neurosci* 18 : 335-346, 2017
- 29) Strange BA, Witter MP, Lein ES, Moser EI: Functional organization of the hippocampal longitudinal axis. *Nat Rev Neurosci* 15 : 655-669, 2014
- 30) Gioia R, Seri T, Diamanti T, et al: Adult hippocampal neurogenesis and social behavioural deficits in the R451C Neuroligin3 mouse model of autism are reverted by the antidepressant fluoxetine. *J Neurochem* 165 : 318-333, 2023
- 31) Khalil MH: Environmental enrichment : a systematic review on the effect of a changing spatial complexity on hippocampal neurogenesis and plasticity in rodents, with considerations for translation to urban and built environments for humans. *Front Neurosci* 18 : 1368411, 2024
- 32) Shoubridge C, Harvey RJ, Dudding-Byth T: IQSEC2 mutation update and review of the female-specific phenotype spectrum including intellectual disability and epilepsy. *Hum Mutat* 40 : 5-24, 2019
- 33) Wickstrom R: Effects of nicotine during pregnancy : human and experimental evidence. *Curr Neuropharmacol* 5 : 213-222, 2007
- 34) Matagne V, Borloz E, Ehinger Y, et al: Severe offtarget effects following intravenous delivery of AAV9-MECP2 in a female mouse model of Rett syndrome. *Neurobiol Dis* 149 : 105235, 2021
- 35) Jeon S, Park J, Likhite S, et al: The postnatal injection of AAV9-FOXP1 rescues corpus callosum agenesis and other brain deficits in the mouse model of FOXP1 syndrome. *Mol Ther Methods Clin Dev* 32 : 101275, 2024
- 36) Toudji I, Toumi A, Chamberland É, Rossignol E: Interneuron odyssey : molecular mechanisms of tangential migration. *Front Neural Circuits* 17 : 1256455, 2023

(2024. 8. 8 received ; 2024. 8. 23 accepted)